

J.S. BADER^{1,✉}
M.W. DEEM²
R.W. HAMMOND¹
S.A. HENCK¹
J.W. SIMPSON¹
J.M. ROTHBERG¹

A Brownian-ratchet DNA pump with applications to single-nucleotide polymorphism genotyping

¹ CuraGen Corporation, 555 Long Wharf Drive, New Haven, CT 06511, USA

² Department of Chemical Engineering, University of California, Los Angeles, CA 90095, USA

Received: 7 November 2001/Accepted: 14 January 2002
Published online: 22 April 2002 • © Springer-Verlag 2002

ABSTRACT We have fabricated a micron-scale device capable of transporting DNA oligomers using Brownian ratchets. The ratchet potential is generated by applying a voltage difference to interdigitated electrodes. Cycling between the charged state and a discharged, free-diffusion state rectifies the Brownian motion of charged particles. The observed macroscopic transport properties agree with the transport rate predicted from microscopic parameters including the DNA diffusivity, the dimensions of the ratchet potential, and the cycling time. Applications to human genetics, primarily genotyping of single-nucleotide polymorphisms (SNPs), are discussed.

PACS 87.10+e; 87.80-Mj; 05.40.-a

1 Introduction

One of the keys to understanding the function of each human gene is to characterize the effect of genetic variations; of greatest medical interest are the genetic factors that predispose individuals to complex diseases including metabolic, cardiovascular, autoimmune, and psychiatric disorders. These functional variants are likely to occur in the coding sequences of genes and include single-nucleotide polymorphisms (SNPs) that result in amino acid changes or frameshift mutations. Rapidly assessing which allele an individual has inherited on each chromosome is a prerequisite for conducting genetic studies, and developing technology that can accomplish this goal rapidly, accurately, and inexpensively is crucial to advancing medical knowledge.

Here we review our design and testing of a micro-machined DNA transport device that could serve as a building block for a highly automated and massively parallel lab-on-a-chip for SNP genotyping [1, 2]. A distinguishing feature of our device is that an electric potential gradient generates a periodic, asymmetric ratchet potential that is sufficiently strong to trap DNA 20-mers to 50-mers, the requisite size range for SNP genotyping. Others have described ratchet potentials formed using electric potential gradients, optical tweezers, and entropic squeezing [3–10], which are sufficiently strong to capture meso-scale particles (kilobases of DNA) but may not be effective for trapping smaller oligomers.

The pertinent details of the device are summarized in Sect. 2, and the macroscopic transport rate is related to microscopic properties. Results are presented in Sect. 3, and a discussion of possible applications is provided in Sect. 4.

2 Methods

Traps for charged particles were generated by depositing two sets of interdigitated platinum electrodes on a silicon surface (Fig. 1). When a solution containing DNA molecules is applied to the device, with a cover slip to prevent evaporation, and a potential difference V is applied to the electrodes, the negatively charged DNA molecules are attracted to the electrodes with positive bias. As shown in the schematic, the positively charged and negatively charged electrode arrays are each periodic over length L , and the two arrays are offset by distance R , defined as the closer edge-to-edge distance, to generate an asymmetric sawtooth-shaped ratchet potential. We fabricated devices with $(L, R) = (50 \mu\text{m}, 5 \mu\text{m})$ and $(20 \mu\text{m}, 2 \mu\text{m})$, with electrode widths $5 \mu\text{m}$ and $2 \mu\text{m}$, respectively. For greater detail regarding the fabrication, see [1] and [2].

When the potential bias is removed, the DNA molecules undergo free diffusion. After time t , the potential bias is reapplied, and the particles that have diffused further than R are transported at least one well. This fraction is denoted α . Assuming a normal density profile characteristic of Brownian motion,

$$\alpha = 1 - \Phi\left(\frac{R}{\sqrt{2Dt}}\right), \quad (1)$$

where $\Phi(z)$ is the cumulative standard normal probability and D is the DNA diffusion constant. With sufficient asymmetry, $L - R > R$, and sufficiently short time t , back-diffusion may be ignored and particles move at most one well per cycle.

The minimum time τ required for re-trapping is calculated by assuming over-damped motion. The terminal velocity for over-damped motion is the ratio of the force $QV/(L - R)$, where Q is the particle charge, to the mass times the friction constant, equal to $k_B T/D$ where $k_B T$ is the thermal energy. This yields

$$\tau = \frac{(L - R)^2 k_B T}{QVD} \quad (2)$$

✉ Fax: +1-203/401-3333, E-mail: jsbader@curagen.com

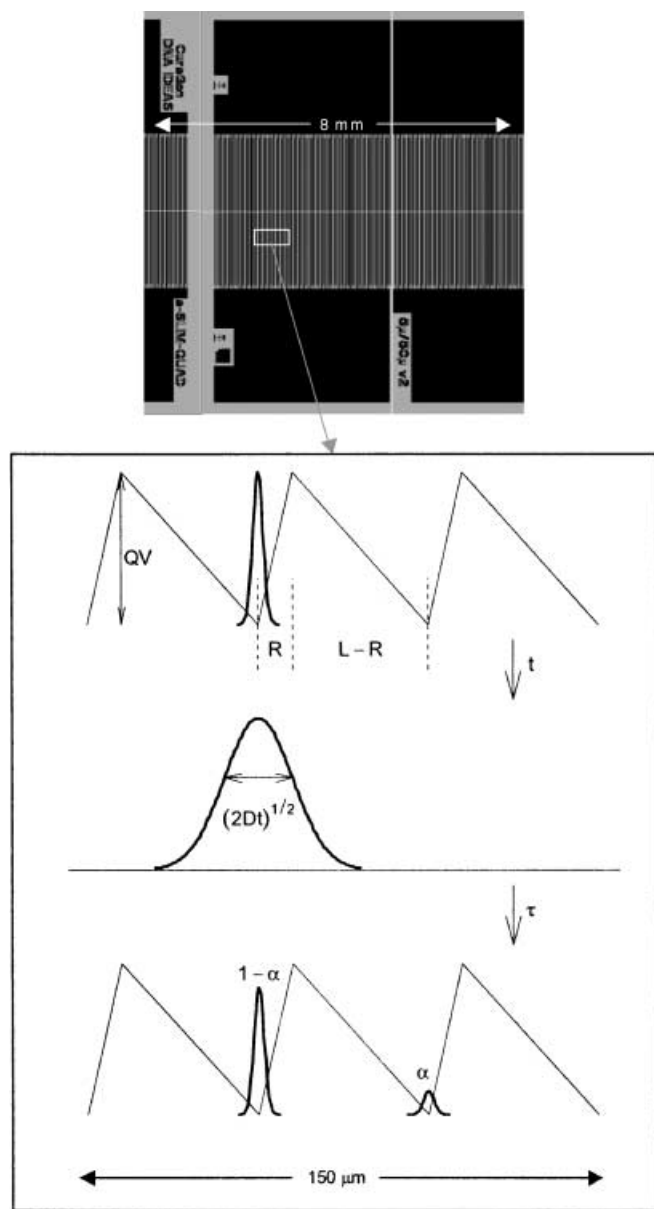


FIGURE 1 *Top:* This mask was used to fabricate devices with $L = 50 \mu\text{m}$ periodicity and $R = 5 \mu\text{m}$ spacing between near electrodes. *Bottom:* A schematic illustrates transport over a cycle of operation. Particles begin trapped in a single well. The potential is turned off for time t , and the particle distribution has a normal density profile with width $(2Dt)^{1/2}$. The potential is re-applied, and after a relaxation time τ the particles are again trapped. A fraction α of the particles have been transported to the next well

for the re-trapping time. In our experiments, the voltage difference was $V = 1.6 \text{ V}$, the thermal energy 26 meV , $QV = 80 \text{ eV}$ for a 50-mer, and $D \approx 1.8 \times 10^{-7} \text{ cm}^2/\text{s}$ (extrapolated from $2.4 \times 10^{-7} \text{ cm}^2/\text{s}$ for a 30-mer near a surface [11]), yielding $\tau = 0.006 \text{ s}$ for the $L = 20 \mu\text{m}$ device.

The flux of particles is $\alpha/(t + \tau) \approx (D/\pi Rt)^{1/2} \exp(-R^2/4Dt)$, the approximation being valid when $\tau < t \leq R^2/2D$. The exponential term arises from the asymptotic expansion for $\Phi(z)$ for large z , $1 - \Phi(z) \sim (2\pi z^2)^{-1/2} \exp(-z^2/2)$. Using this approximation, the flux is maximized for $t \approx R^2/2D$, the time for free diffusion over distance R . An exact numerical solution shows that the true maximum of α/t occurs at $t = 0.35R^2/D$.

The macroscopic transport rate was measured experimentally by cycling the device to transport fluorescently labeled DNA particles to the center, then reversing the polarity of the electrodes to pump the DNA from the center to the ends of the device. Video images recorded the fluorescence intensity over the electrodes during the trapping phase of the cycle, and the images were digitized to extract the DNA concentration at each electrode. Each complete cycle was a square wave with $t = 2\tau$; the frequency of modulation was $(1.5t)^{-1}$.

After n cycles, the mean x_n and variance σ_n^2 of the DNA distribution are given by a binomial distribution with parameter α ,

$$\begin{aligned} x_n &= n\alpha L \\ \sigma_n^2 &= n\alpha(1-\alpha)L^2 \end{aligned} \quad (3)$$

For each experiment, we ascertained that the mean and variance of the DNA distribution grew linearly with cycle number n (see Fig. 2), then obtained α as the slope parameter from a least-squares fit to x_n . The slope of σ_n^2 yields a second estimate for α , which we checked for consistency with the typically more accurate estimate from x_n .

3 Results

The transport properties for single-stranded DNA 50-mers on a device with $(R, L) = (2 \mu\text{m}, 20 \mu\text{m})$ are shown in Fig. 3. Each point is the value of α extracted from the slope of x_n from an independent experiment, and the line is a fit to the anticipated functional form.

The single parameter of the fit is the quantity $(R^2/2D)^{1/2}$, which is found to be 0.52 ± 0.03 . From the residuals of the fit, the standard error for the value of α from each experimental point is 0.04. This agrees well with the mean standard error of 0.05 provided by the least-squares estimator for α .

The corresponding estimate for D is $(3.8 \pm 0.2) \times 10^{-8} \text{ cm}^2/\text{s}$, which is 4.7 times larger than the expected value of $1.8 \times 10^{-7} \text{ cm}^2/\text{s}$ (see Sect. 2). A possible explanation is that DNA molecules are distributed over the entire surface of the electrodes during the trapping phase and, during the free diffusion phase, must travel the center-to-center distance rather than the center-to-edge distance to be transported to the next well. This suggests using $2R = 4 \mu\text{m}$ rather than $R = 2 \mu\text{m}$ in the expression for α and implies a diffusion constant $(1.5 \pm 0.1) \times 10^{-7} \text{ cm}^2/\text{s}$, not significantly different from the expected value.

The transport parameter α is shown as a function of DNA oligomer length in Fig. 4 with results for a 25-mer, a 50-mer, and a 100-mer. Experimental measurements are from devices with $(R, L) = (2 \mu\text{m}, 20 \mu\text{m})$ and $(5 \mu\text{m}, 50 \mu\text{m})$ using free-diffusion time $t = 0.333 \text{ s}$ and trapping time $\tau = 0.167 \text{ s}$. The experimental measurements have been fit to the functional form $\alpha = 1 - \Phi[(R^2/2D_N t)^{1/2}]$, where $D_N = D_{50}(N/50)^\lambda$ is the diffusion constant of an oligomer with N nucleotides, λ is a scaling constant, and D_{50} is the reference diffusion constant for a 50-mer.

The fit value of λ is -0.14 ± 0.06 . The corresponding exponent for a three-dimensional self-avoiding walk is $\lambda = -0.6$. The smaller value we find for λ suggests that the oligomers have not yet entered the scaling regime, either

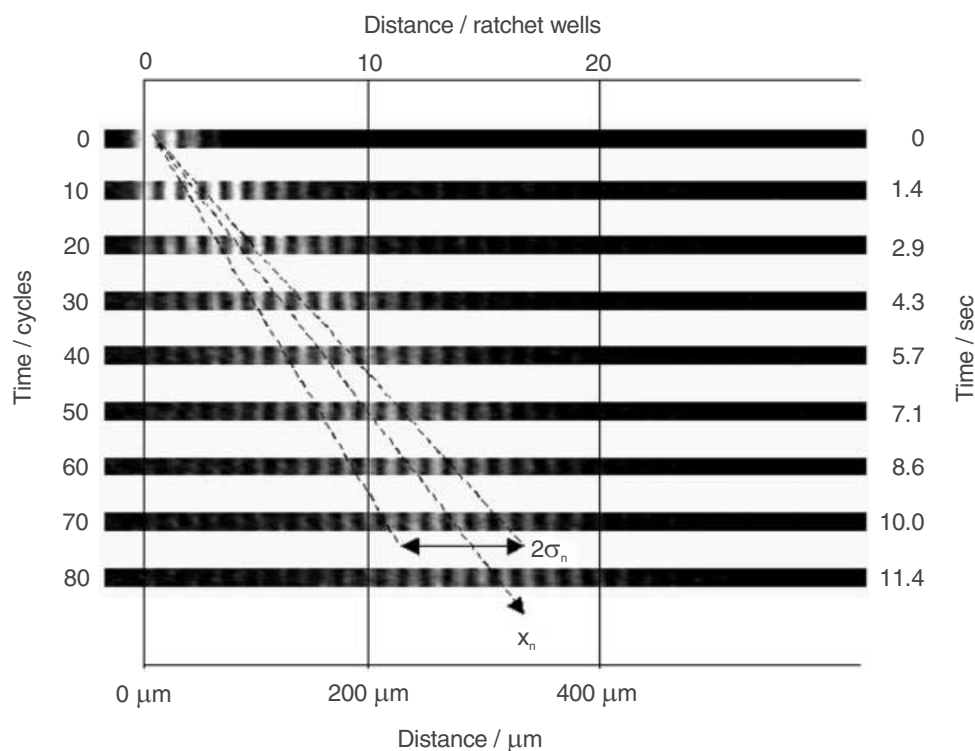


FIGURE 2 Video images captured from transport of a DNA 50-mer on a device with $(R, L) = (2 \mu\text{m}, 20 \mu\text{m})$ are shown every 10 cycles ($t = 0.95 \text{ s}$, $\tau = 0.48 \text{ s}$, $\text{freq} = 0.7 \text{ Hz}$). Superimposed on the images are the mean x_n and the width σ_n of the DNA distribution after n cycles. The transport parameter α is approximately 0.19, and $\sigma_n = 0.39n^{1/2}$

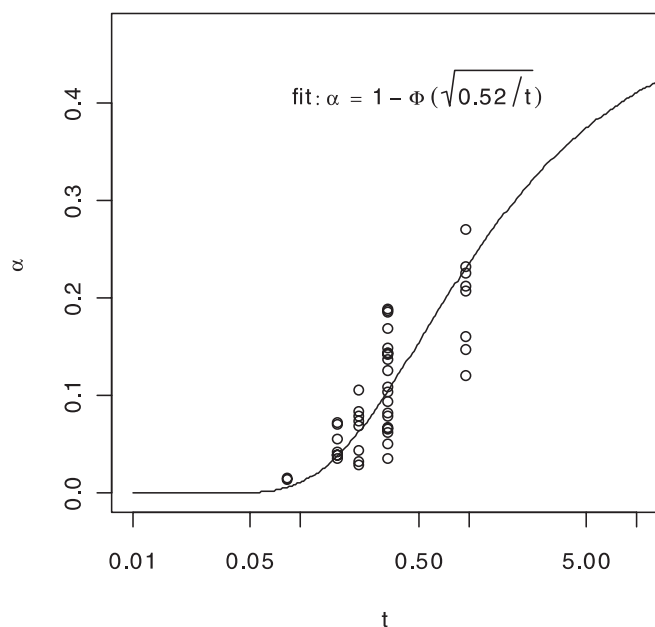


FIGURE 3 The transport parameter α was measured for a DNA 50-mer on a device with $(R, L) = (2 \mu\text{m}, 20 \mu\text{m})$ and fit to the functional form $\alpha = 1 - \Phi[(R^2/2Dt)^{1/2}]$, yielding $R^2/2D = 0.52 \pm 0.03 \text{ s}$

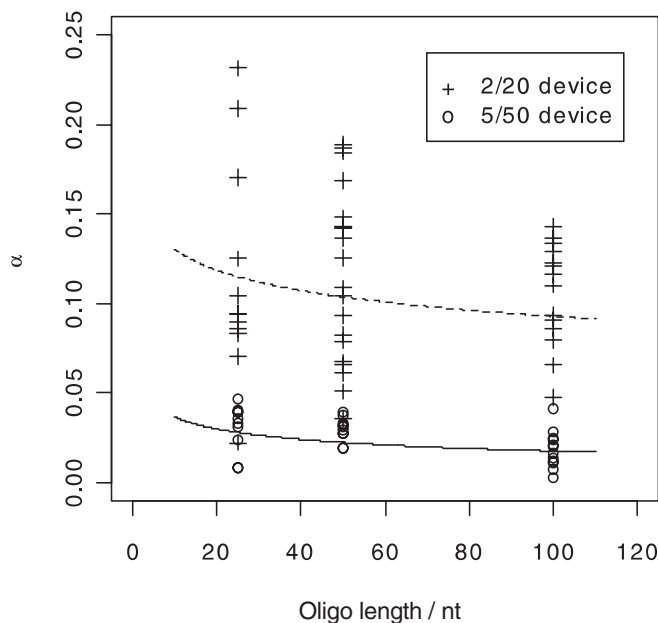


FIGURE 4 Experimental measurements of the transport parameter α as a function of DNA oligomer length are shown for devices with $(R, L) = (2 \mu\text{m}, 20 \mu\text{m})$ and $(5 \mu\text{m}, 50 \mu\text{m})$, free-diffusion time $t = 0.333 \text{ s}$, and trapping time $\tau = 0.167 \text{ s}$. Fits to the functional form $\alpha = 1 - \Phi[(R^2/2Dt)^{1/2}]$ are shown as *dashed* and *solid lines*

due to the contribution of the dye or because the contour length of the oligomer is not much larger than the persistence length. Experimental measurements of single-stranded DNA at high salt concentration (10 mM phosphate buffer, 5 mM MgCl_2) have recently been interpreted to indicate a persistence length of 1.92 nm, corresponding to 2.74 nucleotides with a monomer length of 0.7 nm [12]. Excluding the effects of the dye, the contour lengths of the 25-mer, 50-mer, and 100-mer are 18 nm, 35 nm, and 70 nm, a range of 10–40 times

the persistence length; the radii of gyration, assuming self-avoiding-walk scaling, are 7.2 nm, 11 nm, and 17 nm, respectively. Our experiments were run in zwitterionic 50 mM L-histidine at pH 7.65. The conductivity of this buffer was less than $60 \mu\text{S/cm}$, indicating low ionic strength and suggesting a longer persistence length than in the aforementioned high-salt experiment.

Using the anticipated functional form, adequate fits could be achieved only by allowing D_{50} to depend on the feature size. For the (2 μm , 20 μm) device, $D_{50} = (3.8 \pm 0.5) \times 10^{-8} \text{ cm}^2/\text{s}$, whereas for the (5 μm , 50 μm) device, $D_{50} = (9.3 \pm 1.2) \times 10^{-8} \text{ cm}^2/\text{s}$. The need for different values of D_{50} may result from the simplified one-dimensional treatment of the periodic potential.

In Figs. 3 and 4, the measured values of α have a large spread. While our experiments did not permit a definitive explanation of the sources of variation, two contributing factors may have been run-to-run variations in temperature and in the electrode surface. Temperature variations affect the diffusivity of DNA in aqueous solution: the viscosity of water decreases approximately 2% per Celsius degree at ambient temperature. The DNA molecules adopt a more globular conformation as temperature increases, which may also affect diffusivity. Electrode surface changes may occur due to electrochemical reactions or due to adsorption of DNA or contaminants.

4 Discussion

We have demonstrated that Brownian ratchets can be designed to transport DNA oligomers. The transport rate depends primarily on the diffusion constant of the particles, and a simplified one-dimensional model provides the connection between the microscopic diffusion constant and the macroscopic transport. The diffusion constant implied by the one-dimensional data for transport observed using the device matches known experimental values when the ratchet distance corresponds to the center-to-center distance between trapping electrodes (rather than the edge-to-edge distance). We observe a diffusion constant that scales for DNA of length N nucleotides as $N^{-0.14}$, rather than $N^{-0.6}$, possibly because the 25-mers to 100-mers studied are not yet in the scaling regime. One shortcoming of the one-dimensional model may be that the effective diffusion constant depends on the electrode spacing and the feature size.

A possible application of the device could be DNA genotyping. Since the transport rate of particles depends on their diffusion constant in free solution, the device could be used for size-dependent DNA separations in aqueous buffer. Aqueous buffer provides an advantage over electrophoretic separations that require special media to achieve differential transport rates.

Probing a polymorphic site using a ratchet device could be performed using a pair of genotyping primers flanking the variation. In common genotyping techniques, a 400–500-nucleotide fragment is amplified from genomic DNA prior to genotyping, and a pair of 12 nucleotide primers would be

sufficient to uniquely identify the polymorphic site. An assay could be designed by making the 3' terminal base of one primer overlap with the polymorphic site and using enzymatic specificity to ligate the two primers only when the terminal base is complementary. The assay results could be determined by separating the 12 nucleotide and 24 nucleotide products, using either fluorescently labeled primers or separate reactions to quantify the concentration of each allele.

With the ratchet device, a suitable separation would be achieved when the distance between the 12-mer and 24-mer is equal to the width of the DNA distributions across the electrodes, $|x_n - x'_n| = \sigma_n$, where primed quantities refer to the longer oligomer. Using the expressions for x_n and σ_n provided by (3) and solving for n yields the number of cycles required for a separation,

$$n = \frac{\alpha(1-\alpha)}{(\alpha-\alpha')^2}. \quad (4)$$

Assuming that a device with $(R, L) = (0.1 \mu\text{m}, 1 \mu\text{m})$ could be fabricated, the minimum number of cycles required for a separation is 930, using $t = 1 \times 10^{-3} \text{ s}$ ($\alpha = 0.150$ and 0.138 for the two oligomers). The trapping time τ should be no longer than $1 \times 10^{-3} \text{ s}$, which may be achieved using a 0.1 V potential difference. The total separation time under these assumptions is 2 s. The 12-mer will have traveled 140 wells in this time, and the separation length would be 140 μm .

ACKNOWLEDGEMENTS Portions of this work were supported by the National Human Genome Research Institute Small Business Innovations Research Grant 1 R43 HG01535-01 and by the National Institute of Standards and Technology Advanced Technology Program Award 1996-01-0141. We wish to thank G.A. McDermott, J.M. Bustillo, and G.T. Mulhern for their contributions.

REFERENCES

- 1 J.S. Bader, R.W. Hammond, S.A. Henck, M.W. Deem, G.A. McDermott, J.M. Bustillo, J.W. Simpson, G.T. Mulhern, J.M. Rothberg: Proc. Nat. Acad. Sci. USA **96**, 13 165 (1999)
- 2 R.W. Hammond, J.S. Bader, S.A. Henck, M.W. Deem, G.A. McDermott, J.M. Bustillo, J.M. Rothberg: Electrophoresis **21**, 74 (2000)
- 3 J. Rousselet, L. Salome, A. Ajdari, J. Prost: Nature **370**, 446 (1994)
- 4 L.P. Faucheux, L.S. Bourdieu, P.D. Kaplan, A.J. Libchaber: Phys. Rev. Lett. **74**, 1504 (1995)
- 5 L. Gorre, E. Ioannidis, P. Silberzan: Europhys. Lett. **33**, 267 (1996)
- 6 G.W. Slater, H.L. Guo, G.I. Nixon: Phys. Rev. Lett. **78**, 1170 (1997)
- 7 D. Ertas: Phys. Rev. Lett. **80**, 1548 (1998)
- 8 C.F. Chou, O. Bakajin, S.W. Turner, T.A. Duke, S.S. Chan, E.C. Cox, H.C. Craighead, R.H. Austin: Proc. Nat. Acad. Sci. USA **96**, 13 762 (1999)
- 9 A. van Oudenaarden, S.G. Boxer: Science **285**, 1046 (1999)
- 10 G.A. Griess, E. Rogers, P. Serwer: Electrophoresis **22**, 981 (2001)
- 11 X.-H. Xhu, E.S. Yeung: Science **275**, 1106 (1997)
- 12 A. Montanari, M. Mézard: Phys. Rev. Lett. **86**, 2178 (2001)